National Institute of Physics
Annual Report of the Photonics Research Laboratory
Period covered: 01 January to 31 December 2015

Prepared by

Nathaniel P. Hermosa II, PhD
Program Coordinator
Photonics Research Laboratory
Submitted: 22 January 2016

Contents

1. Executive Summary

1.1. Activities of the research group

1.1.1. Organization

Regular members			3
Student members			18
	PhD students	3	
	MS students	7	
	BS students	8	
Apprentices			3
		Total	24

1.1.2. Mentoring

	Number of graduates
BS Physics	0
BS Applied Physics	2 (2)[1]
MS Physics	2
MS MSE	0
PhD Physics	0
Total	4 (6)

1.2. Research highlights

International peer-reviewed journals	4 (2)[2]
Local peer-reviewed journals	0
International conference papers	2[3]
International conference presentations	2
Local conference papers	26
Local conference presentations	28
Chapter in books	0
Patents	0
NIP funded projects	3
Non-NIP funded projects	3
Major equipment acquired/ upgraded	1
Research travels abroad	4

1 2 students graduated last December 2014. They were not included in the 2014 Photonics Research Laboratory annual report.

2 2 more manuscripts are accepted in 2015. The publication dates are not yet released.

3 The proceedings of SPECKLE 2015 is also indexed in Scopus.

Visiting researchers	3
MOA's entered with local and foreign institutions	0

1.3. Extension work highlights

Extension work activities	6
Research interns/ OJT's for training held at NIP	6

1.4. Main challenges encountered and proposed solutions

1.5. Awards or accreditations received/ positions of responsibility held and other accomplishments

National awards or accreditation received, positions of responsibility held	3
International awards or accreditations received, positions of responsibility held	0
Other accomplishments	0

2. Technical Report

2.1. Activities of the research group

- The Photonics Research Laboratory helped graduate 4 BS students and 2 MS students, and we welcomed a new BS student in the group. The group has 24 research members currently.

- We hosted 3 visiting professor – Prof. Hans Bachor (Australian National University), Dr. Vince Daria (Australian National University) and Prof. Wolfgang Osten () - and 4 of our members have visited research laboratories abroad.

- Dr. Percival Almoro has been awarded the 2014 NRCP Achievement Award in Physics.

- Dr. Percival Almoro had been invited to give a talk at SPECKLE 2015 International Conference on Optical Metrology held last August 24-26 2015 in Guanajuato, Mexico while Dr. Nathaniel Hermosa had a plenary talk at the 33rd SPP Physics Congress, held last 3-6 June, 2015 at the University of Northern Philippines, Vigan, Ilocos Sur, Philippines.

- The group published 1 ISI/SCI indexed journal article and 1 Scopus indexed conference proceeding. 2 ISI/SCI indexed journal articles have been accepted for publication but are still awaiting publication date.

- The group had participated in 3 international conferences. Nestor Bareza Jr presesnted his research at the 11th Conference on Lasers and Electro-Optics Pacific Rim (CLEO-PR) organized by Optical Society of Korea held last August 24-28, 2015 at BEXCO, Busan, Korea while Jessa Jayne Miranda and Joseph de Mesa presented their work at the 7th International Congress on Laser Advanced Material Processing (LAMP) held in Kitakyushu International Conference, Fukuoka, Japan last May 26-29 2015. Dr. Percival Almoro had been invited to give a talk at SPECKLE 2015 International Conference on Optical Metrology held last August 24-26 2015 in Guanajuato, Mexico

- The group presented 26 papers at the SPP Physics congress held last 3-6 June, 2015 at the University of Northern Philippines, Vigan, Ilocos Sur, Philippines ,and joined the National Research Council of the Philippines' Annual General Membership Assembly held last March 11, 2015 at the Philippine International Convention Center, Pasay City. Dr. Nathaniel Hermosa is a plenary speaker at the 33rd SPP Physics Congress.

- Dr. Percical Almoro chaired IllumiNASYON, NIP's symposium on the International Year of Light. Dr. Almoro, Dr. Garcia and Dr. Hermosa gave a talk in this symposium separately.

- Dr. Nathaniel Hermosa and Dr. Percival Almoro continues to be a referees for various optical journals. Dr. Percival Almoro, Dr. Wilson Garcia and Dr. Nathaniel Hermosa reviewed submissions to the 33rd SPP Physics Congress.

2.1.1. Organizations

2.1.1.1. Group members

Regular members (3)

1. Almoro, Percival
2. Garcia, Wilson
3. Hermosa, Nathaniel II

Student members

PhD students (3)

1. Abregana, Timothy Joseph (P2)
2. Dasallas, Lean (P4)
3. De Mesa, Joseph (P1)

MS students (5)

1. Bareza, Nestor Jr. (M2)
2. Engay, Einstom (M1)
3. Escoto, Esmerando (M2)
4. Miranda, Jessa Jayne (M4)
5. Olaya, Cherrie May (M3)

MSE students (2)

1. Amo, Annaliza (M4)
2. Patricio, Floyd Willis (M2)

BS Applied Physics students (5)

1. Doblado, Gerald John (B4)
2. Onglao, Mario III (B5)
3. Sagisi, Jenny Lou (B4)
4. Salcedo, Dylan (B5)
5. Zambale, Nina Angelic (B4)

BS Physics students (3)

1. Emparado, Rommil (B5)
2. Grana, Josemaria (B7)
3. Wang, Maria Ysabel (B3)

2.1.1.2. Apprentices (3)

1. Celerbrado, Michelle (B3)
2. Lofamia, Micherene Clauzette (B3)
3. Narag, Jadze Princeton (M1)

2.1.1.3. Summary

Regular members			3
Student members			18
	PhD students	3	
	MS students	7	
	BS students	8	
Apprentices			3
		Total	24

2.1.2. Mentoring

2.1.2.1. List of graduates

1st semester 2014-2015 (2 BS)

1. Joshua Immanuel Beringuela, BS Applied Physics, December 2014
   Electrical, optical and magnetic properties of low pressure argon and air DC glow discharge plasmas (Adviser: Wilson O. Garcia)

2. Cristina Manejero, BS Applied Physics, December 2014
   Diffuse illumination digital shearography: a wave propagation based model (Adviser: Percival Almoro)

2nd semester 2014-2015 (2 BS, 2 MS)

3. Einstom Engay, BS Applied Physics, June 2015
   Enhanced tomographic reconstruction via multiple-plane phase retrieval and compressive sensing (Adviser: Percival Almoro)

4. Roseanne Novesteras, BS Applied Physics, June 2015
   Shower curtain effect with image enhancement: a wave propagation-based model (Adviser: Percival Almoro)

5. Arriane Lacaba, MS Physics, June 2015
   Femtosecond pulsed laser deposition of Nd:YAG on silicon with nitrogen and oxygen background gases (Adviser: Wilson O. Garcia)

6. Joseph De Mesa, MS Physics, July 2015
   Pulsed laser deposition system for metal oxide film growth (Adviser: Wilson O. Garcia)

2.1.2.2. Summary

	Number of graduates
BS Physics	0
BS Applied Physics	2 (2)[4]
MS Physics	2
MS MSE	0
PhD Physics	0
Total	4 (6)

4 2 students graduated last December 2014. They were not included in the 2014 Photonics Research Laboratory annual report.

2.2. Research highlight

2.2.1. Publication in ISI/SCI and Scopus indexed journals (2 + 2[5])

1. Bareza, N.D. Jr. and N. Hermosa. 2015. “Propagation dynamics of vortices in helico-conical optical beams,” Optics Communications 356:236-242.

2. Almoro, P.F, and T.J. T. Abregana. 2015 “Enhanced axial localization of rough objects using statistical fringe processing algorithm.” In Speckle 2015: VI International Conference on Speckle Metrology, pp. 96600F-96600F. International Society for Optics and Photonics, 2015.

3. Hermosa, N. 201x. “Reflection beamshifts of visible light due to graphene.” *Accepted in Journal of Optics. Institute of Optics, 2015.*

4. De Mesa, J.A. et al. 201x. “Effects of deposition pressure and target-substrate distance on growth of ZnO by femtosecond pulsed laser deposition.” A*ccepted in Journal of Laser Micro/Nanoengineering. 2015.*

2.2.2. Publication in local peer reviewed journals (0)

2.2.3. International conference papers (2)

1. Almoro, P.F, and T.J. T. Abregana. 2015 “Enhanced axial localization of rough objects using statistical fringe processing algorithm.” In Speckle 2015: VI International Conference on Speckle Metrology, pp. 96600F-96600F. International Society for Optics and Photonics, 2015. [6]

2. Bareza Jr, N., and N. Hermosa. “Spatial mode projection technique in extracting nanofeatures.” In Conference on Lasers and Electro-Optics/ Pacific Rim, p. 27P_20. Optical Society of America, 2015.

2.2.4. International conference presentations (2)

1. De Mesa, J.A., A.C. Amo, L.V. Sayson, J.J. Miranda, R.V. Sarmago, and W.O. Garcia. 2015. "Study of morphological properties and elemental microcomposition of ZnO grown by femtosecond pulsed laser deposition." Paper presented in the 7th International Congress on Laser Advanced Materials Processing, Kitakyushu, Japan, May 26-29. Japan: Japan Laser Processing Society.

2. Miranda, J.J., J.A. De Mesa, and W.O. Garcia. 2015. "Optical emission spectroscopy of femtosecond pulsed laser produced aluminum plasma." Paper presented in the 7th International Congress on Laser Advanced Materials Processing, Kitakyushu, Japan, May 26-29. Japan: Japan Laser Processing Society.

5 Manuscript accepted by 2015 but no publication date yet.
6 The proceedings of SPECKLE 2015 is also indexed in Scopus.

2.2.5. Local conference papers

2.2.5.1. With full paper (26)

1. Abregana, T.T. and P.F. Almoro. 2015. "Effects of object spatial frequency on the performance of the multiple-plane phase retrieval method." In Proceedings of the Samahang Pisika ng Pilipinas: 33rd Physics Congress, Vigan City, 03-06 June 2015, SPP – 2015 – PA – 03.

2. Bareza, N.D. Jr., E. Escoto, and N. Hermosa. 2015. "Measurement of orbital angular momentum of light by polygon apertures." In Proceedings of the Samahang Pisika ng Pilipinas: 33rd Physics Congress, Vigan City, 03-06 June 2015, SPP – 2015 – 5A – 05.

3. Bareza, N.D. Jr, and N. Hermosa. 2015. "Detecting multiple optical vortices numerically." In Proceedings of the Samahang Pisika ng Pilipinas: 33rd Physics Congress, Vigan City, 03-06 June 2015, SPP – 2015 – PB – 07.

4. Calleja, M., J. Miranda, and W.O. Garcia. 2015. "Graphite films grown via fs pulsed laser deposition at different temperatures." In Proceedings of the Samahang Pisika ng Pilipinas: 33rd Physics Congress, Vigan City, 03-06 June 2015, SPP – 2015 – PB – 21.

5. Dasallas, L.L. A.P. Lacaba, and W.O. Garcia. 2015. "Effect of substrate heat treatment on femtosecond pulsed laser deposited Nd:YAG films." In Proceedings of the Samahang Pisika ng Pilipinas: 33rd Physics Congress, Vigan City, 03-06 June 2015, SPP – 2015 – PB – 19.

6. Dasallas, L.L., R.B. Jaculbia, M. Balois, W. Garcia, and N. Hayazawa. 2015. "Imaging and orientational properties of single molecule detected by a high NA objective lens." In Proceedings of the Samahang Pisika ng Pilipinas: 33rd Physics Congress, Vigan City, 03-06 June 2015, SPP – 2015 – 1A – 03.

7. De Mesa, J.A., A.C. Amo, H. Salazar, J.J. Miranda, R.V. Sarmago, and W.O. Garcia. 2015. "Catalyst-free deposition of ZnO nanorods on silicon (1000 using femtosecond pulsed laser deposition in oxygen background gas." In Proceedings of the Samahang Pisika ng Pilipinas: 33rd Physics Congress, Vigan City, 03-06 June 2015, SPP – 2015 – 3C – 05.

8. De Mesa, J.A., A.M. Amo, H. Salazar, J.J. Miranda, R.V. Sarmago, and W.O. Garcia. 2015. "Growth of ZnO on silicon (100) with oxygen background gas using femtosecond pulsed laser deposition." In Proceedings of the Samahang Pisika ng Pilipinas: 33rd Physics Congress, Vigan City, 03-06 June 2015, SPP – 2015 – PA – 15.

9. Doblado, G.H., N.D. Bareza Jr, and N. Hermosa. 2015. "Goos-Hanchen and Imbert-Fedorov shifts induced by silver, gold and copper." In Proceedings of the Samahang Pisika ng Pilipinas: 33rd Physics Congress, Vigan City, 03-06 June 2015, SPP – 2015 – PB – 08.

10. Emperado, R.B., J.L.B. Saguisi, J.I.I. Beringuela, and W.O. Garcia. 2015. "Spatially-resolved spectroscopic measurements on the regions of an argon DC glow discharge." In Proceedings of the Samahang Pisika ng Pilipinas: 33rd Physics Congress, Vigan City, 03-06 June 2015, SPP – 2015 – 3A – 01.

11. Engay, E. and P.F. Almoro. 2015. "Tomographic reconstruction based on phase retrieval and compressive sensing." In Proceedings of the Samahang Pisika ng Pilipinas: 33rd Physics Congress, Vigan City, 03-06 June 2015, SPP – 2015 – 3A – 03.

12. Engay, E., M. Jamerlan, R. Novesteras, and N. Hermosa. 2015. "Wavefront engineering for advanced undergraduate optics class." In Proceedings of the Samahang Pisika ng Pilipinas: 33rd Physics Congress, Vigan City, 03-06 June 2015, SPP – 2015 – PA – 41.

13. Escoto, E.R. and P.F. Almoro. 2015. "Gaussian filters for off-axis digital holography via angular spectrum method." In Proceedings of the Samahang Pisika ng Pilipinas: 33rd Physics Congress, Vigan City, 03-06 June 2015, SPP – 2015 – PB – 02.

14. Escoto, E.R., R.A. Novesteras, and P.F. Almoro. 2015. "Multiple-plane iterative phase retrieval for objects hidden around a corner or behind a diffuser." In Proceedings of the Samahang Pisika ng Pilipinas: 33rd Physics Congress, Vigan City, 03-06 June 2015, SPP – 2015 – PA – 04.

15. Grana, J.R. and W.O. Garcia. 2015. "Unknotting of chains on a vibrating platform." In Proceedings of the Samahang Pisika ng Pilipinas: 33rd Physics Congress, Vigan City, 03-06 June 2015, SPP – 2015 – PA – 37.

16. Hermosa, N. 2015. "Reflection beamshifts of visible light due to graphene." In Proceedings of the Samahang Pisika ng Pilipinas: 33rd Physics Congress, Vigan City, 03-06 June 2015, SPP – 2015 – PA – 05.

17. Jaculbia, R.B., N. Hayazawa, L. Dasallas, M. Balois, and S. Kawata. 2015. "Imaging and polarization properties of CdSe quantum dot at an interface detected by a high NA objective lens." In Proceedings of the Samahang Pisika ng Pilipinas: 33rd Physics Congress, Vigan City, 03-06 June 2015, SPP – 2015 – PA – 02.

18. Lacaba, A.P., F.W.I. Patricio, A.C. Amo, L.L. Dasallas, and W.O. Garcia. 2015. "Structural and morphological characterization of Nd:YAG on silicon (100) grown by femtosecond pulsed laser deposition with nitrogen and oxygen background gases." In Proceedings of the Samahang Pisika ng Pilipinas: 33rd Physics Congress, Vigan City, 03-06 June 2015, SPP – 2015 – PA – 21.

19. Miranda, J.J., J.A. De Mesa, and W.O. Garcia. 2015. "Optical emission spectroscopy of femtosecond pulsed laser produced aluminum plasma." In Proceedings of the Samahang Pisika ng Pilipinas: 33rd Physics Congress, Vigan City, 03-06 June 2015, SPP – 2015 – PA – 20.

20. Novesteras, R. and P.F. Almoro. 2015. "Enhanced images via shower curtain effect using adhesive tapes." In Proceedings of the Samahang Pisika ng Pilipinas: 33rd Physics Congress, Vigan City, 03-06 June 2015, SPP – 2015 – PB – 03.

21. Olaya, C.M.M., R. Emperado, L.Dasallas, and W.O. Garcia. 2015. "Density measurement in helium glow discharge using absorption spectroscopy." In Proceedings of the Samahang Pisika ng Pilipinas: 33rd Physics Congress, Vigan

City, 03-06 June 2015, SPP – 2015 – 4B – 03.

22. Onglao, M.S. and P.F. Almoro. 2015. "Correction of multiple optical vortices." In Proceedings of the Samahang Pisika ng Pilipinas: 33rd Physics Congress, Vigan City, 03-06 June 2015, SPP – 2015 – PB – 05.

23. Onglao, M.S. and P.F. Almoro. 2015. "Image encryption by visual cryptography with error analysis." In Proceedings of the Samahang Pisika ng Pilipinas: 33rd Physics Congress, Vigan City, 03-06 June 2015, SPP – 2015 – 1A – 05.

24. Patricio, F.W.I., A.P. Lacaba, L.L. Dasallas, and W.O. Garcia. 2015. "Surface topographical analysis of Er:YAG on silicon grown by femtosecond pulsed laser deposition" In Proceedings of the Samahang Pisika ng Pilipinas: 33rd Physics Congress, Vigan City, 03-06 June 2015, SPP – 2015 – PA– 16.

25. Sabanal, S., M. Bondoc, and N. Hermosa. 2015. "Controllable Bessel-like beams self-reconstruct", In Proceedings of the Samahang Pisika ng Pilipinas: 33rd Physics Congress, Vigan City, 03-06 June 2015, SPP – 2015 – Pa – 01.

26. Zambale, N.A.F., N.D. Bareza Jr, and N. Hermosa. 2015. "Optical beam generation via incoherent superposition of phases." In Proceedings of the Samahang Pisika ng Pilipinas: 33rd Physics Congress, Vigan City, 03-06 June 2015, SPP – 2015 – 5A – 01.

2.2.5.2. Without full paper (2)

1. Hermosa, N. 2015. "Optical beams endowed with orbital angular momentum: generation, some new application, and outlook", Plenary talk at the Samahang Pisika ng Pilipinas: 33rd Physics Congress, Vigan City, 03-06 June 2015.

2. Lacaba, A., J. De Mesa, F. W. I. Patricio, L. Dasallas, and W. Garcia. 2015. “Deposition of Nd:YAG on Silicon using Femtosecond Pulsed Laser Deposition with Oxygen Background Gas.” Paper presented at National Research Council of the Philippines’ Annual General Membership Assembly, Pasay City, 11 March 2015.

3. Almoro, P, 2015. “Holograms using tunable diffuse light.” Paper presented at *IlumiNASYON: International Year of Light*, NIP Auditorium, 09 March 2015.

4. Garcia, W, 2015. “Light pulses for spectroscopy and waveguides.” Paper presented at *IlumiNASYON: International Year of Light*, NIP Auditorium, 09 March 2015.

5. Hermosa, N II, 2015. “Seeing things in a new light.” Paper presented at IlumiNASYON: *International Year of Light, NIP Auditorium*, 09 March 2015.

2.2.6. Chapter in books (0)

2.2.7. Patents (0)

2.2.8. NIP funded projects (3)

Almoro, Percival	Digital shearography with diffuse illumination	01 January – 31 December 2015
Garcia, Wilson	Pulsed laser deposition of novel materials	01 January – 31 December 2015
Hermosa, Nathaniel	Coherent beam superposition with incoherent addition of holograms	01 January – 31 December 2015

2.2.9. Non-NIP funded projects (3)

Project proponent	Project title	Period	Amount	Project grantor
Hermosa, Nathaniel	Establishment of a structured light laboratory within the Photonics Research Laboratory of the National Institute of Physics	01 July 2015 – 30 June 2017	PhP 2, 500,000.00	OVPAA UP System
Hermosa, Nathaniel	Development of a fast and inexpensive phase front sensor using a digital micromirror device to determine the phase front and the Poynting vector skew angle of optical fields with complex amplitudes	01 July 2015 – 30 June 2016	PhP 300,000.00	OVCRD Outright grant UP Diliman
Garcia, Wilson	Atomic Absorption Spectroscopy of Laser-produced Plasma	01 October 2014 – 20 September 2015	PhP 300,000.00	OVCRD UP Diliman

2.2.10. Major equipment acquired

Equipment	Cost	Source of fund	Project proponent
Texas Instruments, Digital Micromirror Display (2)	PhP 90, 450.00	OVCRD Outright grant, UP Diliman	Nathaniel Hermosa

2.2.11. Research travels abroad

NIP Personnel	Purpose	Place	Dates	Mode of exchange
Almoro, Percival	Visit in foreign research lab	Centro Investigationes Optic (CIO), Leon, Mexico	27 August 2015	Arranged by host for foreign speakers
Bareza, Nestor Jr. Dasallas, Lean L. Escoto, Esmerando	Summer School on Lasers and Laser Applications	Asian Laser Center, Advanced Photonics Research Institute, Gwangju Institute of Science and Technology	06 – 11, July 2015	Arranged by host , competitive application

2.2.12. Visiting researchers

Visitor	Date of visit	NIP Personnel/ Contact person	Mode of exchange
Bachor, Hans	23 – 24 April 2015	Nathaniel Hermosa	Arranged by NIP-PRL
Daria, Vince	April – June 2015	Nathaniel Hermosa	Balik Scientist DOST, Arranged by NIP-PRL and SPP
Osten, Wolfgang	1 June 2015	Percival Almoro	Arranged by NIP-PRL and SPP

2.2.13. MOA's entered with local or foreign institutions (0)

2.3. Extension work highlights

2.3.1. Extension work activities (6)

Almoro, Percival	Referee, various optical journals
Almoro, Percival	Topical editor for optics and photonics, 33rd SPP Physics Congress. Reviewer for optics.
Almoro, Percival	Resource speaker for mentoring during NAST-sponsored research upgrading workshops. Invited by NAST.
Garcia, Wilson	Reviewer for optics, photonics and plasma physics, 33rd SPP Physics Congress.
Hermosa, Nathaniel	Referee, Optical Society of America journals
Hermosa, Nathaniel	Topical editor for optics and photonics, 33rd SPP Physics Congress, Reviewer for optics and physics education papers.

2.3.2. Research interns/OJT's (6)

SSIP	Charles Bartolo Philippines Science High School – Central Luzon Campus
	Levi Gamba Philippines Science High School – Bicol Region Campus
	Kevin Gines Philippines Science High School – Cordillera Administrative Region Campus
	Sean Derrick Navarro Philippines Science High School – Ilocos Region Campus
DOST-OJT	Dina Grace Banguilan, BS Physics University of Northern Philippines, Vigan
	Christine Ann Faraon, BS Physics Polytechnic University of the Philippines, Manila

2.4. Main challenges encountered and proposed solutions

The schedule to receive the interns and OJT's conflict with the schedule of classes at NIP.

2.5. Awards or accreditation received/ positions of responsibility held

2.5.1. National (3)

Percival Almoro	Chair, NIP Symposium, "IlumiNASYON: International Year of Light".
Percival Almoro	2014 NRCP Achievement Award for Physics
Wilson Garcia	President, Samahang Pisika ng Pilipinas

2.5.2. International (0)
2.5.3. Other accomplishments (0)

3. Photons, ISI/SCI publications and other appendices

3.1. Photos

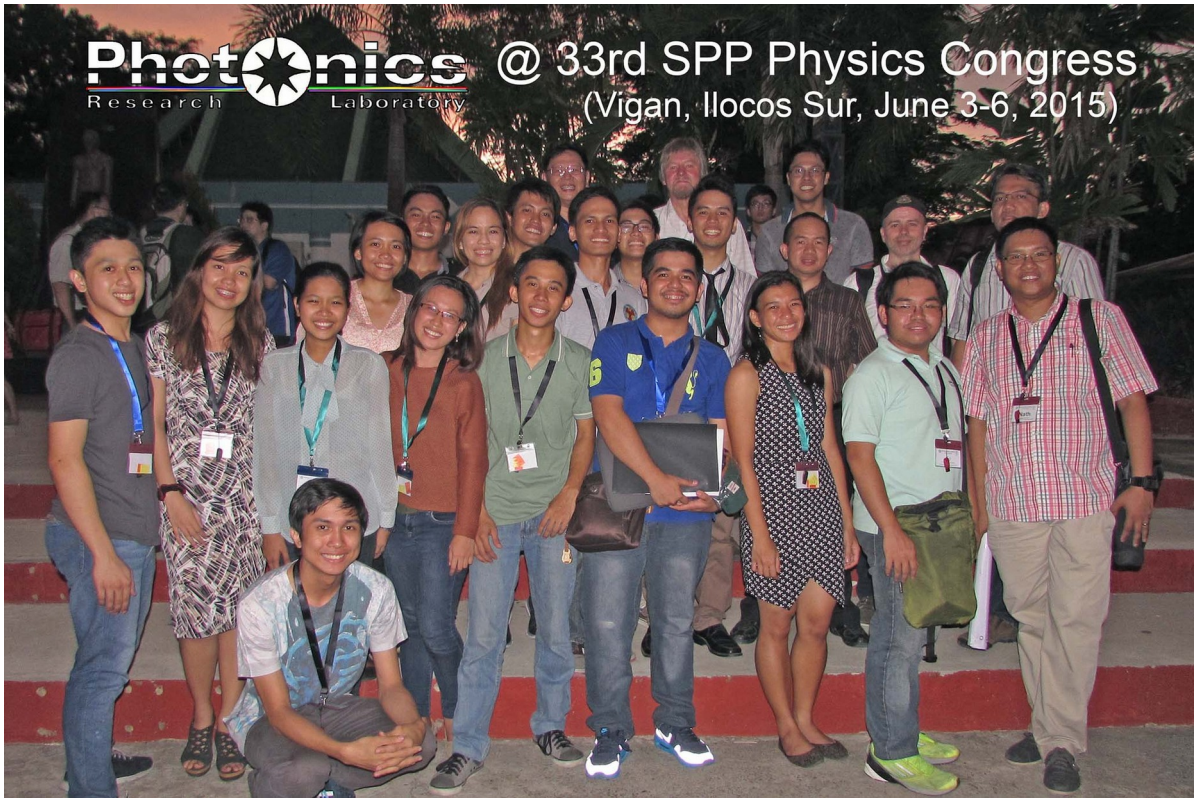

PHOTONICS GROUP (Feb. 16, 2015, Univ. of the Philippines Diliman, QC)

3.2. ISI/SCI/ Scopus publications

1. Bareza, N.D. Jr. and N. Hermosa. 2015. “Propagation dynamics of vortices in helico-conical optical beams,” Optics Communications 356:236-242.

2. Almoro, P.F, and T.J. T. Abregana. 2015 “Enhanced axial localization of rough objects using statistical fringe processing algorithm.” In Speckle 2015: VI International Conference on Speckle Metrology, pp. 96600F-96600F. International Society for Optics and Photonics, 2015.

Optics Communications 356 (2015) 236–242

Contents lists available at ScienceDirect

Optics Communications

journal homepage: www.elsevier.com/locate/optcom

Propagation dynamics of vortices in helico-conical optical beams

Nestor Bareza Jr.*, Nathaniel Hermosa

National Institute of Physics, University of the Philippines, Diliman, Quezon City 1101, Philippines

ARTICLE INFO

Article history:
Received 29 May 2015
Received in revised form
16 July 2015
Accepted 4 August 2015

Keywords:
Optical vortices
Wave propagation
Laser beam shaping

ABSTRACT

We present the dynamics of optical vortices (OVs) that came from the propagation of helico-conical optical beam. This dynamics is investigated numerically by tracking the OVs at several distances using rigorous scalar diffraction theory. To ensure that our numerical calculations are correct, we compare the intensity profiles and their corresponding interferograms taken at different propagation distances between simulations and experiments. We observe that the peripheral isopolar vortices transport radially inward, toward the optical axis along the transverse spatial space as the beam propagates. When the beam has a central vortex, these vortices have significant induced angular rates of motion about the optical axis. These propagation dynamics of vortices influence the internal energy flow and the wave profile reconstruction of the beam, which can be important when deciding their applications.

1. Introduction

An optical vortex (OV), first described in the seminal work of Nye and Berry, is a region of singularity in which the wave amplitude vanishes and the phase is indeterminate [1]. Wavefronts that contain OV include Laguerre–Gaussian beams [2] and higher order Bessel beams [3], as well as their fractional counterparts [4,5]. An underlying interest on these kinds of beams emerges since OV carries orbital angular momentum. These beams also have wide range of potential applications such as in information encoding, free-space information transfer [6], optical trapping [7] and micromanipulation [8].

The study of the dynamics of OV may offer substantial explanations to other related physical phenomena such as drift events, gyration and hydrodynamics [9,10]. Thus, there is a demand to understand the dynamical behavior of OV. OV has fluid-like motion as the beam propagates which is explained by the potential theory [11]. For multiple OVs in a single beam, same-charge (isopolar) vortices are found to gyrate together while opposite-charge (bipolar) vortices tend to drift away from the direction of beam axis [9]. Investigating dynamical behavior of three or more OVs in a single beam has not been fully explored. Although Roux derived mathematical expressions for interaction of two OVs [9], several complications arise in providing a preliminary model for interacting three or more OVs. This kind of system, which cannot be described by mutual interactions such as 2-body mechanics problem and 2-charge electrodynamics problem, requires statistical approach [12,13].

Helico-conical optical beam (HCOB) is a special type of beam which can produce a string of multiple OVs when propagated. The HCOB is an interesting beam in that it acquires OVs as it propagates because of its peculiar phase: it has inseparable azimuthal θ and radial ρ phases. HCOB phase $\phi(\rho, \theta)$ is expressed as

$$\phi(\rho, \theta) = l\theta\left(K - \frac{\rho}{\rho_o}\right) \tag{1}$$

where l is the topological charge, ρ_o normalizes ρ, and K can take the value of either 0 or 1. HCOB has been observed to generate a string of l isopolar peripheral OVs and has an oppositely l-charged central vortex for K equal to 1 [14]. These same polarity OVs in the radial opening are interacting which cause angular and radial phase variations [15]. Their interactions cause the rotations of OVs as the beam propagates which affects the intensity profile. In this paper, we report the first detailed study of dynamical behavior of a string of multiple OVs in HCOB as the beam propagates. We presented the interaction of peripheral OVs with and without the presence of central OV. This is based on the radial and angular motions of OVs in beam profiles that are obtained at fine-scaled propagation distances.

Several approaches in OV detection have been demonstrated numerically and experimentally, in which some are discussed in the following. Roux performed a numerical closed line integral to the gradient of the phase profile in locating the OV [9]. A closed line integral to a continuous gradient results to a zero value. Hence, an integral which results to a non-zero value implies that it is evaluated at discontinuous region, which indicates that inside the contour is an OV. Maallo and Almoro demonstrated detection

* Corresponding author.
E-mail address: nbareza@nip.upd.edu.ph (N. Bareza Jr.).

http://dx.doi.org/10.1016/j.optcom.2015.08.005
0030-4018/

of single OV by the axial behavior in retrieved phase maps [16]. They based their detection on the behavior of OV which has rapid phase variation in the transverse space and has phase invariance along axial direction. Murphy et al. experimentally located OVs using a Shack–Hartmann wavefront sensor [17]. The slopes in the acquired wavefront surface are used in an algorithm to display branch point potential map in which peaks and valleys display both the locations and polarities of the OVs. Ricci et al. used multi-pinhole interferometry to demonstrate the vortex-splitting phenomenon that is able to detect OV when 2D scanning is performed [18]. In our study, it is necessary that multiple OVs can be detected simultaneously even at relatively far propagation distance. Also, intensity profiles obtained at fine-scaled propagation distances are needed to closely track the motion of OVs, which is difficult to achieve experimentally. Numerical approach provides a noise-free system and may generate significant interaction characteristics between the OVs at fine-scaled propagation distances. The numerical closed line integral used by Roux and the algorithm based on axial behavior developed by Maallo and Almoro both require scanning before OV can be detected. Hence, we utilized a numerical simulation that is able to detect multiple OVs simultaneously at a fine-scaled propagation distance even as far as 1000 mm. The locations of OVs can be determined by getting the intersection of the zeroes of the real and imaginary parts of the complex wave amplitude profile. The validity of numerical results was verified by comparing it to experimental results.

The observation of the dynamical behavior of OVs in HCOB may find potential applications to a more controllable micromanipulation or optical spanner by just adjusting the phase parameters, or a better understanding of reconstruction characteristics of the self-healing property of HCOBs [19].

2. Experiment and simulations

We present the experimental methods and the simulation steps in this section. Fig. 1 illustrates the experimental setup. A collimated HeNe laser (wavelength $\lambda = 632.8$ nm) passes through a computer-generated hologram (CGH) which is placed at the front focal plane of the first lens $L1$ ($f1 = 500$ mm). The production of CGH is described elsewhere [20].

Intensity of HCOB beam that contains the OVs is acquired experimentally based on the holographic setup used in [20]. The beam diffracts into different orders after passing through the CGH. HCOB intensity profile can be obtained from the 1st order which is selected by an aperture that is placed at the back focal plane of $L1$. A second lens $L2$ is positioned beyond the aperture at a distance equivalent to its focal length ($f2 = 250$ mm). A CCD camera is placed right after the back focal plane of $L2$. The camera captures the near field intensity patterns of the HCOB. We also open the aperture to accommodate the zeroth order so that superposing this with the 1st order will yield interferograms. Interferograms are produced to verify the relative polarities and the magnitudes of OVs. Illustration of the quantification of topological charges by interferograms and confirming the topological charge conservation are presented in [21].

Rigorous scalar diffraction theory is utilized for propagating the HCOB numerically. The phase expression given by Eq. (1) is used as input function of the beam and the wavelength used is 633 nm. A complex wave function representing the electric field is acquired after propagation at a set distance. HCOB vortices are located by the intersection between zeroes of real part and imaginary part of the complex electric field. The OVs are located for several propagation distances so that OVs' motions in the transverse spatial structure as the beam propagates can be examined. The propagated functions are obtained from 0.1 mm up to 1000 mm propagation distances with 0.1 mm interval. Lastly, the interferograms can also be generated in simulation by superposing HCOB beams with a plane wave. These interferograms are compared to interferograms that are acquired experimentally in order to examine the agreement between experiment and numerical simulation. Detailed discussion of OV detection technique is presented in the next section.

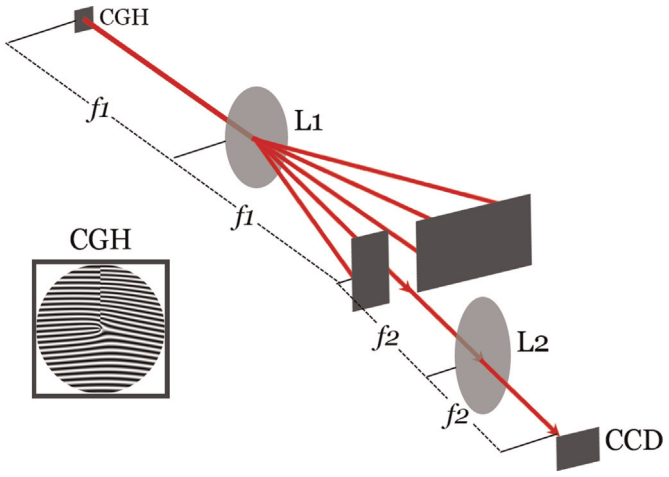

Fig. 1. Experimental setup. The inset shows a computer-generated hologram (CGH) which was constructed digitally and printed on a mask. The beam splits into different orders after passing through the CGH. Then, the 1st order of diffraction which contains HCOB intensity profile is selected by an aperture. The 2nd lens L_2 images the beam onto the CCD camera.

3. Detecting optical vortices numerically

A 1024×1024 pixels frame size is used in the numerical simulation. The side length of this frame is set to 0.8 cm. A circular function whose radius is 0.35 cm is multiplied to initial input function to serve as the initial beam size. By propagating the initial function at a certain distance, a complex wave amplitude profile is obtained.

The OVs are then located by getting the intersection of the zeroes of real and imaginary parts of the complex field. In the numerical simulation, range of values below a chosen threshold pixel value is assigned as zero-valued regions for both the real and imaginary parts. If the threshold value is selected to be very small, we can possibly acquire a single pixel of intersection. This is true for relatively short propagation distances. However, the dark regions on the beam, which correspond to the locations of OVs, expand as the beam propagates. This can be observed in the beams shown in Figs. 2, 3 and 4 which are propagated at 1.0 cm, 20.0 cm and 80.0 cm distances, respectively. Thus, for relatively farther propagation distances, enlarged dark regions yield more clustered points of intersection and some inevitably resulted with unconnected points of intersection.

The threshold value for assigning zeroes of real and imaginary parts should be the same for the entire range of propagation distances to achieve uniformity in parameters. We selected the threshold value to be 0.05 which is observed to adequately yield points of intersection. One issue at relatively farther propagation distances is the occurrence of unconnected points of intersection that signify the same OV. This is resolved by performing image dilation in which a square with 5-pixeled side is used as structure element to dilate the non-zero valued pixels in the array [22]. The image dilation expands a single pixel into the same size of the structure element which enables the connection of unconnected pixels. Since the study aims to observe the dynamical behavior of

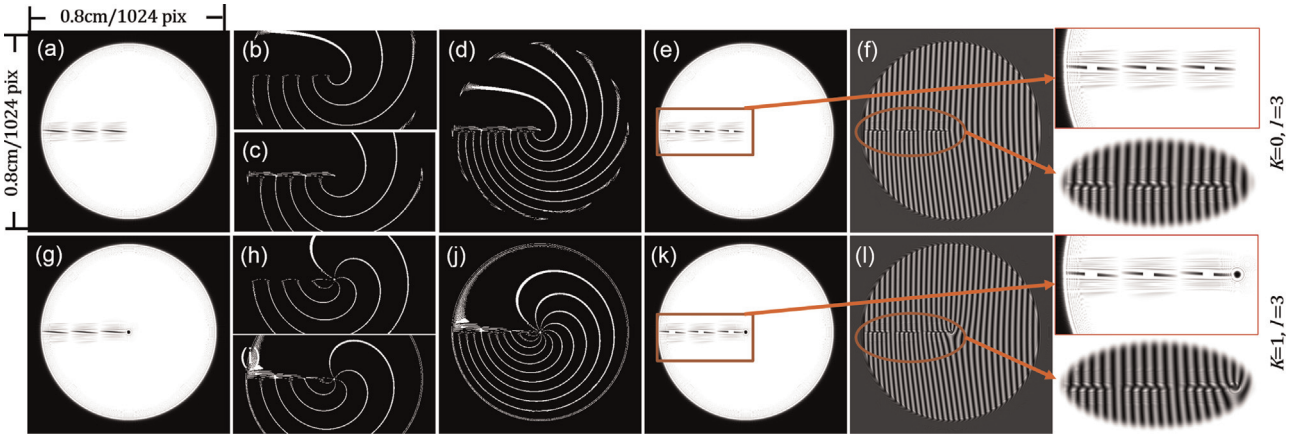

Fig. 2. OV detection in HCOB beam with $l=3$ and [1st *row images*] $K=0$ or [2nd *row images*] $K=1$ propagated at $z=1.0$ cm. The sequence of images from left to right illustrates the (a, g) intensity profiles, zeroes of (b, h) [*upper image*] real part and (c, i) [*lower image*] imaginary part of the complex wave amplitude profile, (d, j) overlain parts, (e, k) detected OVs, and (f, l) interferograms.

OVs as far as 1000 mm propagation distance, some resulting unconnected points are much dispersed which require repetition of image dilation. Hence, image dilation is repeated 5 times to ensure the connection of the points and this is done for all the propagation distances for uniformity.

This study requires detection of multiple OVs in a single beam, hence it is helpful to distinguish groups of pixels that signify different OVs. This is done via blob analysis which is a standard image processing when observing dynamics of certain features in an image [23,24]. Blob analysis starts with binarized image containing blobs or cluster of connected points. These blobs are assigned with different pixel values for distinction, so that analysis or calculations per blob can be performed. In this work, the regions of interest in the image are the vortices which correspond to dark regions in the beam intensity profile. The blobs in this study are the groups of connected pixel points that signify different OVs. One blob can be isolated in the image by calling its corresponding pixel value. The centroid of the blob yields the specific location of an OV. From the coordinates of the centroid, the angular location about the optical axis and radial distance from the optical axis of the OV can be obtained. This calculation is done for locating all the peripheral OVs at different propagation distances. We first demonstrate the OV detection in Fig. 2. The HCOB phase parameters used are $l=3$ and [1st row images] $K=0$ or [2nd row images] $K=1$ propagated at $z=1.0$ cm.

Three peripheral OVs along the left horizontal discontinuous cut can be noticed for both $K=0$ (Fig. 2a) and $K=1$ (Fig. 2g). The branching orientations of the zeroes between $K=0$ (Fig. 2b and c) and $K=1$ (Fig. 2h and i) display hints of the polarities of the OVs. For $K=0$, the branches from the peripheral OVs tend to repel from each other. On the other hand in the presence of a central OV ($K=1$), the branches from peripheral OVs tend to join at the central OV. This indicates that branches of zeroes tend to repel from branch of an OV with same polarity but tend to be attracted to branch of an OV with opposite polarity. The polarities are verified by the fork orientations in the interferograms (Fig. 2f and l). Peripheral OVs have same polarity while the central OV is opposite in polarity because of its flipped fork orientation. The overlain zeroes of real and imaginary parts are shown in Fig. 2d and j. The intersection from these overlain parts is processed with image dilation and blob analysis. The resulting blobs have detected the OVs as shown in Fig. 2e and k. Note that in Fig. 2k, the central OV has no corresponding blob since it is masked in the numerical simulation because of the observed location invariance of this OV as the beam propagates. The purpose of removing the blob for central OV is for simplicity during iteration of OV detection at fine-scaled propagation distances. OV detection is also performed at propagation distance of 20.0 cm as illustrated in Fig. 3.

The dark regions on the intensity beam profiles enlarge as the beam propagates from 1.0 cm (Fig. 2a and g) to 20.0 cm (Fig. 3a and g). This infers that as the beam propagates it is expected that intersecting zeroes of real and imaginary parts will result to more

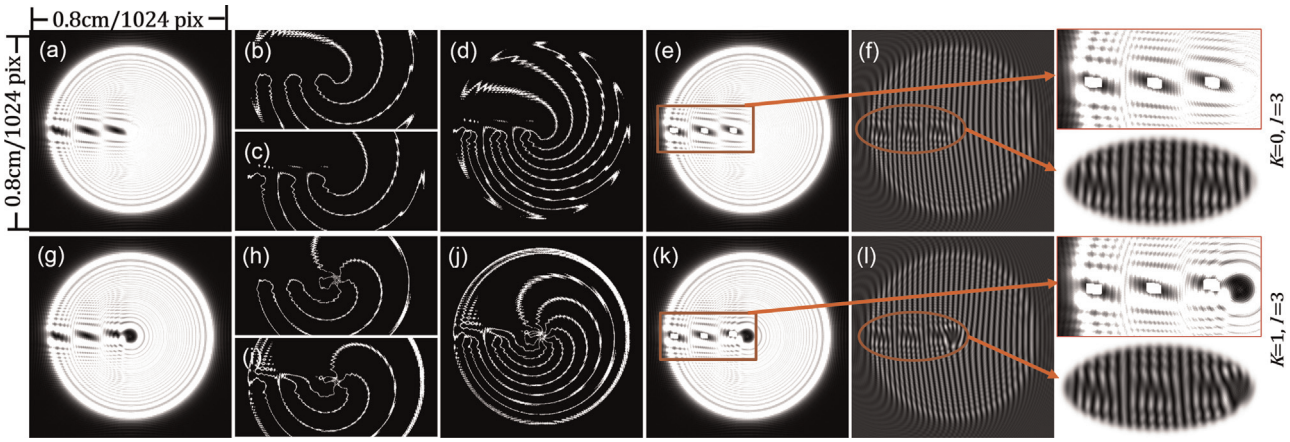

Fig. 3. OV detection in HCOB beam with $l=3$ and [1st *row images*] $K=0$ or [2nd *row images*] $K=1$ propagated at $z=20.0$ cm. The sequence of images from left to right illustrates the (a, g) intensity profiles, zeroes of (b, h) [*upper image*] real part and (c, i) [*lower image*] imaginary part of the complex wave amplitude profile, (d, j) overlain parts, (e, k) detected OVs, and (f, l) interferograms.

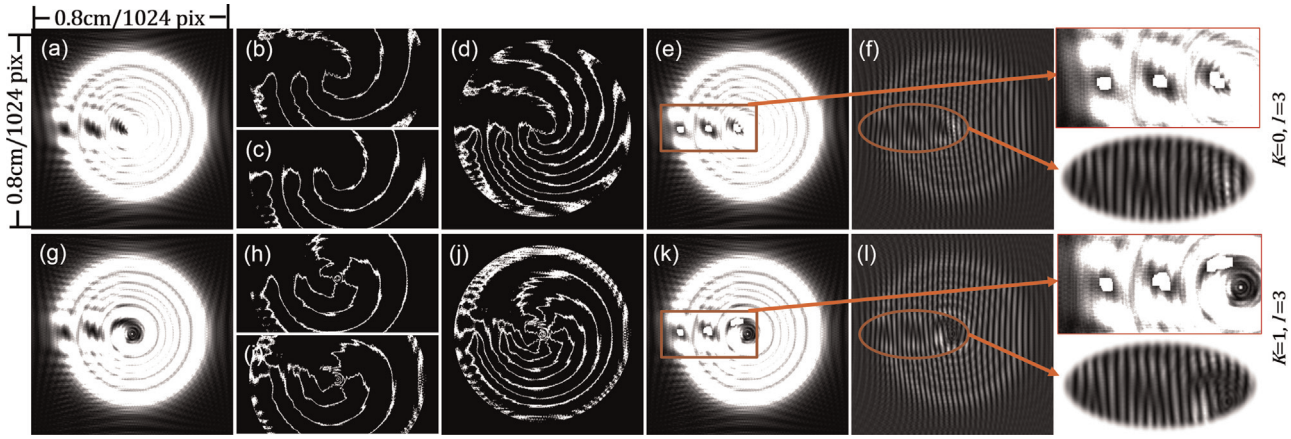

Fig. 4. OV detection in HCOB beam with $l=3$ and [1st *row images*] $K=0$ or [2nd *row images*] $K=1$ propagated at $z=80.0$ cm. The sequence of images from left to right illustrates the (a, g) intensity profiles, zeroes of (b, h) [*upper image*] real part and (c, i) [*lower image*] imaginary part of the complex wave amplitude profile, (d, j) overlain parts, (e, k) detected OVs, and (f, l) interferograms.

cluster of points. This is apparent to the blob sizes in Fig. 3e and k after performing image dilation and blob analysis. The 5 repetition of image dilation is useful in this case to connect more distant clustered points yielding larger blobs. The polarities of OVs are consistent to previously observed (same polarities of peripheral OVs that are opposite to the polarity of central OV) from both the branching orientations in the zeroes of complex wave profile shown in Fig. 3b, c, h and i and the fork orientations in interferograms shown in Fig. 3f and l.

The 5 repetition of image dilation is advantageous for beam propagated at farther distance such as this case since the dark regions become larger. The consistency of the branching orientations in the zeroes and the fork orientations in interferograms reveal that the polarities of the OVs do not change as the beam propagates which is expected.

The technique discussed could detect multiple OVs in a single beam even for farther propagation distances. In the data acquisition, we iterated the OV detection in terms of propagation distances within the range of 0.1 mm up to 1000 mm with 0.1 mm interval. This shows that the technique can be used in studying behavioral dynamics of multiple OVs in a single beam at fine-scaled propagation distances.

4. Results and discussion

4.1. Comparison: experimental and numerical results

We compare the experimental and numerical beam intensity with phase parameters l and K set to 3 and 1, respectively, in Fig. 5. We display the intensity profiles acquired at several propagation distances (near $f2$, ~13 cm from $f2$, and ~27 cm from $f2$). The near field intensity results between experiment and simulation display similar features. Discontinuous cuts are present along the left horizontal region of the intensity profiles. The cut is noticeably consisting of three peripheral vortices that are aligned to the central vortex. These dark spots enlarge through propagation. The peripheral vortices have eccentricities increasing and major axis slanting as the beam propagates. These evolutions reveal the dynamical behavior of the localized vortices which develop into

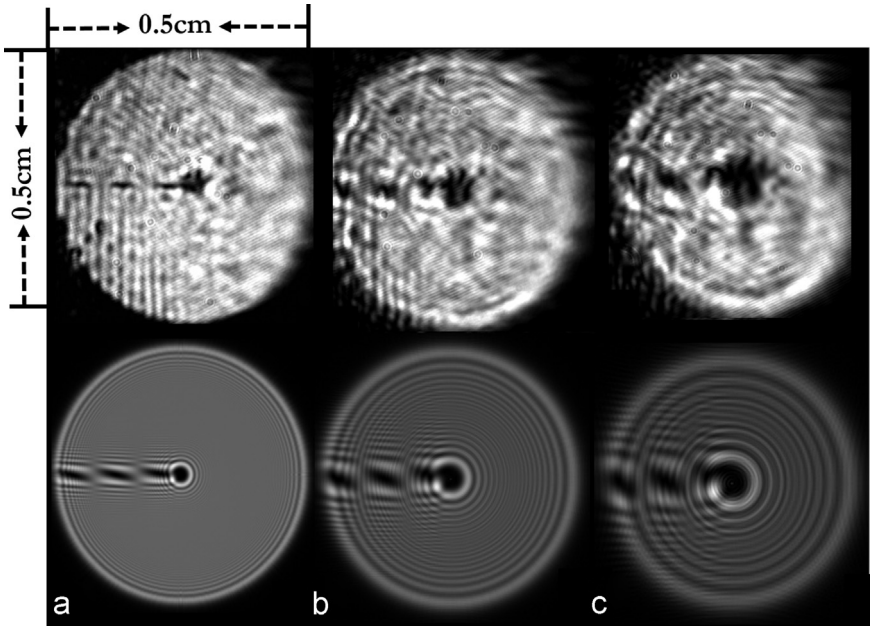

Fig. 5. Comparison of intensity profiles obtained experimentally (images above) and numerically (images below) for propagation distances (a) near focus $f2$ of 2nd lens, (b) ~13 cm from $f2$ and (c) ~27 cm from $f2$.

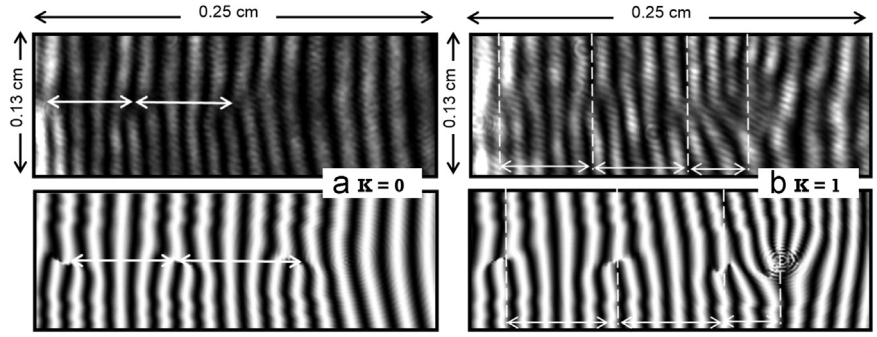

Fig. 6. HCOB interferograms captured experimentally (images above) and obtained numerically (images below) for $K=0$ and $K=1$.

spiralling intensity at the far field as observed by Alonzo et al. [25].

The comparison of experimental and numerical interferograms for both 0 and 1 values of K is shown in Fig. 6. The central nodes of fork holograms display the locations of the vortices while the arm orientations reveal the polarities. The central nodes that correspond to locations of OVs are noticeably aligned peripherally along a single azimuth. The charges of peripheral vortices on both cases are isopolar which is evident by the identical fork orientations. For K equal to 1, the presence of a central vortex whose charge is opposite to the peripheral vortices can be seen. As pertinent to arm counts of fork patterns, the charges of peripheral vortices are all equally 1 while the central vortex is charged 3.

We observed the same correspondence between experimental results and numerical simulation for different values of l ($l=1, 2, 3$) and K ($K=0, 1$). This indicates that our numerical simulations indeed describe what is being observed.

4.2. Simulations: propagation dynamics of OVs

We illustrate the propagation dynamics of the OVs by location maps. In a location map, the propagation distance axis is projected onto 2D transverse spatial space as indicated by the grayscale values of pixels. Relatively darker pixel dot represents OV location for relatively farther propagation distance. A resulting single pixel dot in the location map indicates that the OV has invariant transverse location or it is not moving along beam propagation.

Fig. 7 shows the location maps of three peripheral OVs for both K equal to 0 and 1 with l equal to 3. The farthest propagation distance projected in these maps is 1.0 m. These location maps illustrate the dynamics of peripheral OVs in the left horizontal discontinuous cut in Fig. 5. The maps of peripheral OVs are labelled as *near*, *intermediate* and *far* in reference to their radial distances from optical axis. These maps are magnified with the scale shown also in Fig. 7. No location map is drawn for central OV in the case of $K=1$ since it is observed to be steadily located at the center of the beam. It is evident from the location maps of peripheral OVs that there are dynamical changes in positions of the OVs as the beam propagates.

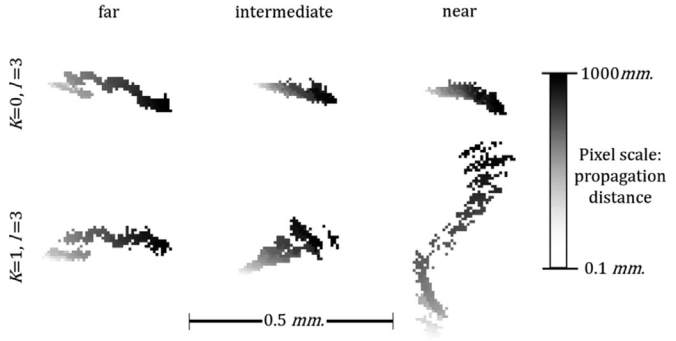

Fig. 7. Location maps. The propagation axis is projected onto 2D transverse spatial space as the grayscale value of the pixels, with relatively darker pixel as relatively farther propagation distance. In the layout are the location maps of peripheral OVs for $l=3$ and $K=0, 1$.

Two pertinent observations can be extracted from these location maps. First, the vortices are perceived to get attracted toward the optical axis. Second, although not so apparent for farther OVs, the direction of angular displacement is opposite between K equal to 0 and 1. Significant angular displacements can be examined for the case K equal to 1, particularly to the *intermediate* and *near* vortices. The nearer vortices tend to be azimuthally displaced at faster rate. This indicates the stronger interaction of relatively nearer vortex to the oppositely charged central vortex. The motion of these OVs can be verified mathematically in the same manner as Roux derived the change in location $r(\rho, \theta)$ of an OV with respect to propagation distance z. By evaluating the gradient of the general expression of HCOB phase given by Eq. (1) with an added factor of $-kz$ where k is the wavenumber, the change in location $\vec{r}(\rho, \theta)$ becomes

$$\frac{d\vec{r}(\rho,\theta)}{dz} = \hat{e_z} + \frac{l\vec{\rho}\times\hat{e_z}}{k\rho^2}\left(K - \frac{\rho}{\rho_o}\right) - \frac{l\theta\vec{\rho}}{\rho\rho_o} \tag{2}$$

where $\hat{e_z}$ and $\vec{\rho}$ denote the unit vector along propagation axis and the separation vector, respectively. Separation vector points to the OV location at (ρ, θ) coordinate. Note that this expression can describe the interaction of two OVs by setting $\vec{\rho}$ as the difference between vectors defining the locations of two OVs with respect to optical axis. Since no simple mathematical model can describe motion of interacting multiple OVs such as three or more, we can treat Eq. (2) to approximately describe motion of each OV independently. The existence of the OV as the beam propagates is ensured by the 1st term in (2). The 2nd and 3rd terms designate the angular and radial behaviors of OV, respectively. The negative sign in the 3rd term confirms the inward motion of OVs. The 2nd term reveals that some angular displacements of peripheral OVs can be observed with ($K=1$) or without ($K=0$) the central OV. Moreover, the direction of angular displacement is opposite between beams with and without the central OV. These angular behavior of OVs are observed in the location maps.

The location maps are helpful for visualizing motion of OVs in the transverse spatial space as the beam propagates. To closely examine with quantitative analysis, the location maps are decomposed to plots comprising the radial and angular displacement versus the propagation distance as presented in Figs. 8 and 9, respectively.

For the case of $l=3$ and $K=0$, all 3 peripheral OVs are found to have inward motion as can be observed from upper plots in Fig. 8 wherein the net radial distances decrease after 1.0 m propagation. This result agrees with the radial change of location with respect to propagation distance given by Eq. (2). Similarly for $l=3$ and

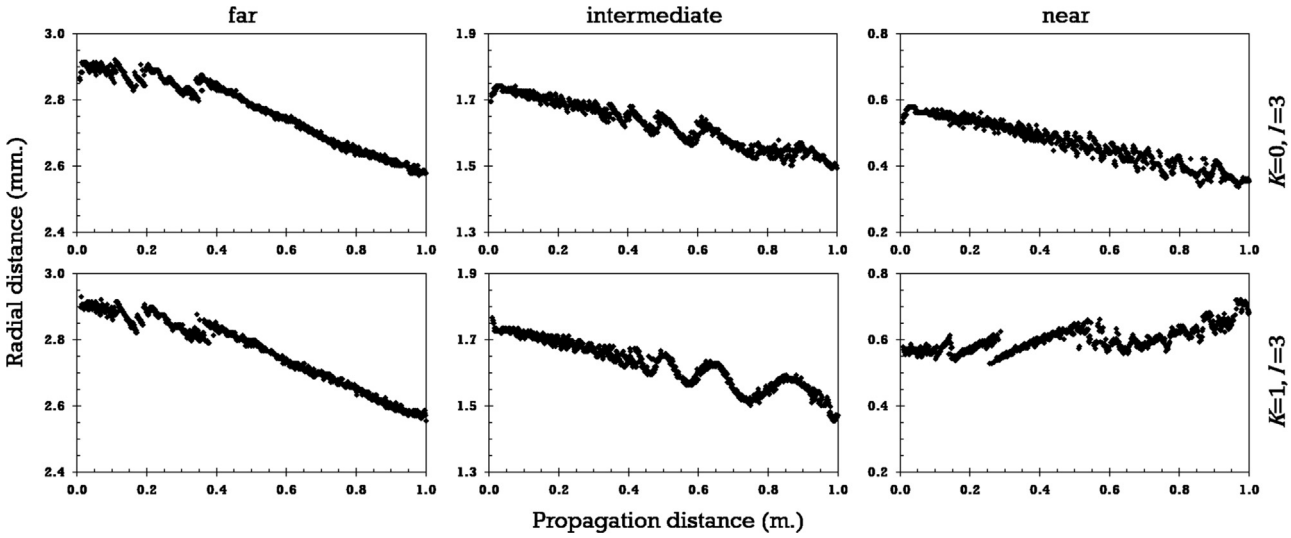

Fig. 8. Radial motion. Plots of radial distance versus propagation distance of peripheral OVs for $l=3$ and $K=0, 1$.

$K=1$, peripheral OVs have inward motion except for the *near* OV as shown by lower plots in Fig. 8. Both results indicate that peripheral OVs are somewhat attracted towards the optical axis except for the *near* OV in $K=1$. The radial plots between K equal to 0 and 1 display almost the same trends for both *intermediate* and *far* OVs. On the other hand, the trends in radial plots of the *near* OV differ between K equal to 0 and 1, in which dynamics of *near* OV is influenced by the presence of a central OV. These observations infer that the presence of strongly charged central OV greatly influences the dynamics of nearest OV neighbor and negligibly affects the dynamics of the farthest OV neighbor. Lastly, we remark on the radial behavior when undulation is observed in the *intermediate* OV for both K equal to 0 and 1. This can be interpreted as the push–pull induced motion to an OV (*intermediate*) due to the OVs (*near* and *far*) that surround it. This undulation cannot be modelled by Eq. (2) and an interaction term between the OVs may be warranted. The dynamics of the OVs, especially the *near* OV, are further investigated for angular displacements as the beam propagates.

In the absence of a central OV ($K=0$), the peripheral OVs tend to have positive azimuthal displacements as apparent in the trends of the upper plots in Fig. 9. However, the angular displacements for *intermediate* and *far* OVs are minute compared to pertinent net angular displacement for *near* OV after 1.0 m propagation. The higher degree of net angular displacement of *near* OV compared to *intermediate* and *far* OVs is also observed in the case with the presence of a central OV ($K=1$) as can be seen in the lower plots in Fig. 9. It can also be noticed that the directions of angular displacements of OVs between K equal to 0 and 1 are opposite. The observed reverse direction is expected as the sign in 2nd term in the expression (2) switches when we set K to either 0 or 1. The results manifest that *near* OV, either with or without a central OV, tend to be angularly displaced at higher magnitude compared to farther OVs. The central OV is strongly interacting with the nearest OV neighbor. The strongly charged central OV prevents the inward motion but heightens the gyration of *near* OV.

We also investigated the dynamics of peripheral OVs for higher l values such as 4, 5 and 6, in which similar results compared to l equal to 3 are observed. Inward motion toward the optical axis is seen for peripheral OVs for either K equal to 0 or 1. The directions of angular displacements of peripheral OVs are opposite between HCOBs with central OV and without central OV. It is also observed for HCOBs with higher l values that the presence of central OV triggers the inward motion and induces significant angular displacement to the nearest peripheral OV. We inspected in l equal to 4 that the undulation also occurred in the intermediate peripheral

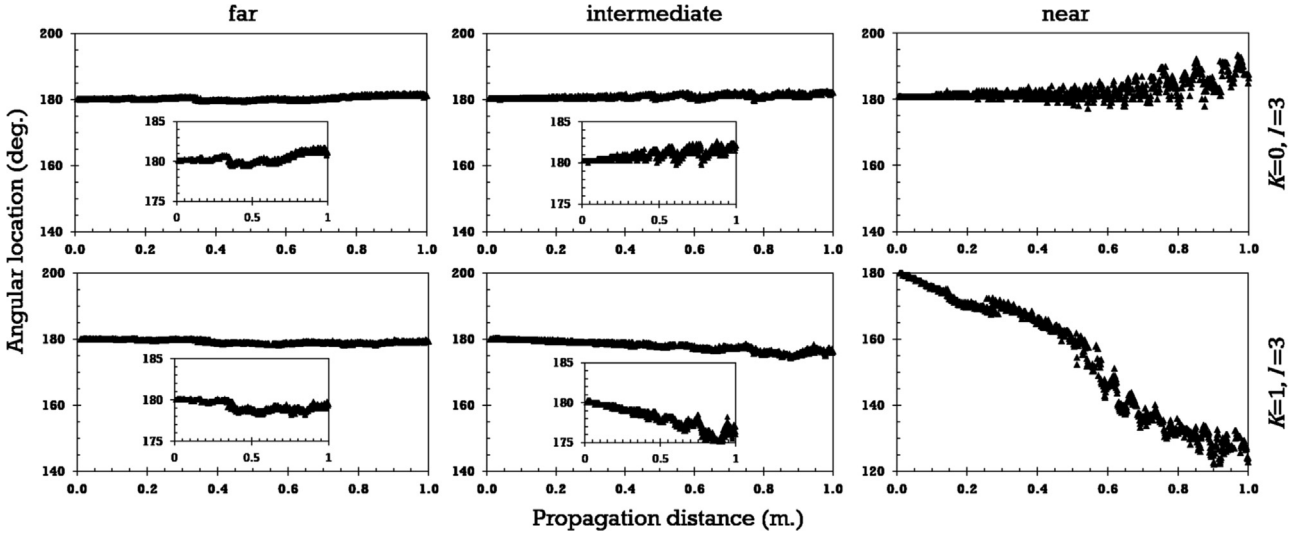

Fig. 9. Angular motion. Plots of angular location versus propagation distance of peripheral OVs for $l=3$ and $K=0, 1$

OVs but with lower amplitude and higher frequency. However, as l value goes higher such as 5 and 6, this undulation becomes less apparent. Moreover for higher l values, the farther the OV from the optical axis the less it is affected by the presence of a central OV since it is observed that direction of angular displacement of this OV is same with the case for no central OV. The dynamics of more peripheral OVs is beyond the scope of this study, although it will be interesting to investigate and detail the behavior.

5. Summary and conclusion

Peripheral OVs of HCOB as the beam propagates are observed to have dynamical behavior in the transverse spatial space. The dynamics is examined by the plots of radial distance and angular displacement versus the propagation distance. Inward motion toward the optical axis is observed for the peripheral OVs as the beam propagates for both K equal to 0 and 1. The direction of angular displacement is opposite between beams with and without a central OV. The nearest OV to optical axis has relatively higher net angular displacements compared to farther OVs as observed for both the case K equal to 0 and 1. Peculiar result is investigated for *near* OV in case of $K=1$ because it strongly interacts with the central OV. Different from the rest peripheral OV, the *near* OV is found to have heightened angular motion about the strongly charged central OV. The gyration of peripheral OVs with incurred inward motion as the beam propagates explain the spiral intensity distribution of HCOB at the far field. This propagation dynamics can be helpful for a more controllable rotational positioning of asymmetrical particles.

Acknowledgment

N. Hermosa received a relocation grant as a Balik Ph.D. from the Office of the Vice President for Academic Affairs, UP system.

References

[1] J. Nye, M. Berry, Dislocations in wave trains, Proc. R. Soc. Lond. A: Math. Phys. Eng. Sci. 336 (1974) 165–190.
[2] L. Allen, M.W. Beijersbergen, R. Spreeuw, J. Woerdman, Orbital angular momentum of light and the transformation of Laguerre–Gaussian laser modes, Phys. Rev. A 45 (11) (1992) 8185.
[3] K. Volke-Sepulveda, V. Garcés-Chávez, S. Chávez-Cerda, J. Arlt, K. Dholakia, Orbital angular momentum of a high-order bessel light beam, J. Opt. B: Quantum Semiclassical Opt. 4 (2) (2002) S82.
[4] S.H. Tao, W.M. Lee, X. Yuan, Experimental study of holographic generation of fractional bessel beams, Appl. Opt. 43 (1) (2004) 122–126.
[5] J.B. Götte, K. O'Holleran, D. Preece, F. Flossmann, S. Franke-Arnold, S. M. Barnett, M.J. Padgett, Light beams with fractional orbital angular momentum and their vortex structure, Opt. Express 16 (2) (2008) 993–1006.
[6] G. Gibson, J. Courtial, M. Padgett, M. Vasnetsov, V. Pas' ko, S. Barnett, S. Franke-Arnold, Free-space information transfer using light beams carrying orbital angular momentum, Opt. Express 12 (22) (2004) 5448–5456.
[7] D. Cojoc, V. Garbin, E. Ferrari, L. Businaro, F. Romanato, E. Di Fabrizio, Laser trapping and micro-manipulation using optical vortices, Microelectron. Eng. 78 (2005) 125–131.
[8] W. Lee, X.-C. Yuan, W. Cheong, Optical vortex beam shaping by use of highly efficient irregular spiral phase plates for optical micromanipulation, Opt. Lett. 29 (15) (2004) 1796–1798.
[9] F.S. Roux, Dynamical behavior of optical vortices, J. Opt. Soc. Am. B 12 (7) (1995) 1215–1221.
[10] M. Vaupel, K. Staliunas, C. Weiss, Hydrodynamic phenomena in laser physics: modes with flow and vortices behind an obstacle in an optical channel, Phys. Rev. A 54 (1) (1996) 880.
[11] D. Rozas, Z. Sacks, G. Swartzlander Jr., Experimental observation of fluidlike motion of optical vortices, Phys. Rev. Lett. 79 (18) (1997) 3399.
[12] F. Ahmad, W.C. Saslaw, N.I. Bhat, Statistical mechanics of the cosmological many-body problem, Astrophys. J. 571 (2) (2002) 576.
[13] C.-T. Sah, W. Shockley, Electron–hole recombination statistics in semiconductors through flaws with many charge conditions, Phys. Rev. 109 (4) (1958) 1103.
[14] N.P. Hermosa, C.O. Manaois, Phase structure of helico-conical optical beams, Opt. Commun. 271 (1) (2007) 178–183.
[15] B.K. Singh, D. Mehta, P. Senthilkumaran, Vortices in helico-conical beam and fractional vortex beam, in: 2013 Workshop on Recent Advances in Photonics (WRAP), IEEE, 2013, pp. 1–2.
[16] A.M.S. Maallo, P.F. Almoro, et al., Numerical correction of optical vortex using a wrapped phase map analysis algorithm, Opt. Lett. 36 (7) (2011) 1251–1253.
[17] M. Kevin, D. Burke, N. Devaney, C. Dainty, Experimental detection of optical vortices with a Shack–Hartmann wavefront sensor, Opt. Express 18 (15) (2010).
[18] F. Ricci, W. Löffler, M. van Exter, Instability of higher-order optical vortices analyzed with a multi-pinhole interferometer, Opt. Express 20 (20) (2012) 22961–22975.
[19] N. Hermosa, C. Rosales-Guzmán, J. Torres, Helico-conical optical beams self-heal, Opt. Lett. 38 (3) (2013) 383–385.
[20] S. Chávez-Cerda, M. Padgett, I. Allison, G. New, J.C. Gutiérrez-Vega, A. O'Neil, I. MacVicar, J. Courtial, Holographic generation and orbital angular momentum of high-order Mathieu beams, J. Opt. B: Quantum Semiclassical Opt. 4 (2) (2002) S52.
[21] L. Stoyanov, S. Topuzoski, I. Stefanov, L. Janicijevic, A. Dreischuh, Far field diffraction of an optical vortex beam by a fork-shaped grating, Opt. Commun. 350 (2015) 301–308.
[22] R.M. Haralick, S.R. Sternberg, X. Zhuang, Image analysis using mathematical morphology, IEEE Trans. Pattern Anal. Mach. Intell. (4) (1987) 532–550.
[23] J. Carbary, K. Liou, A. Lui, P. Newell, C. Meng, "Blob" analysis of auroral substorm dynamics, J. Geophys. Res.: Space Phys. (1978–2012) 105 (A7) (2000) 16083–16091.
[24] P. Telagarapu, M.N. Rao, G. Suresh, A novel traffic-tracking system using morphological and blob analysis, in: 2012 International Conference on Computing, Communication and Applications (ICCCA) , IEEE, 2012, pp. 1–4.
[25] C. Alonzo, P.J. Rodrigo, J. Glückstad, Helico-conical optical beams: a product of helical and conical phase fronts, Opt. Express 13 (5) (2005) 1749–1760.

Enhanced Axial Localization of Rough Objects Using Statistical Fringe Processing Algorithm

Percival F. Almoro and Timothy Joseph T. Abregana
National Institute of Physics, University of the Philippines, Quezon City, Philippines, 1101

Abstract. Fringe patterns carry valuable spatio-temporal information about the object being investigated. Fringe processing, however, is hampered by the presence of speckle noise which is a by-product of coherent metrology of optically rough surfaces. A speckle noise-robust fringe processing algorithm we developed based on the statistical properties of fringe patterns is revisited. The algorithm evaluates the change in the standard deviation of fringe patterns yielding a 2-D contrast map of spatial frequencies along the transverse directions. Application of the algorithm along the axial direction has not been reported. Here a technique for enhanced axial localization of rough test objects based on the statistical fringe processing algorithm is demonstrated experimentally. The main advantages of the localization technique are robustness against speckle noise and high axial resolution in the range of the light source wavelength.

Keywords: wavefront, fringe pattern, holography, phase retrieval, speckle, interferogram

Address all correspondence to: Percival F. Almoro, National Institute of Physics, University of the Philippines, Quezon City, Philippines, 1101; Tele-Fax: +632 9209749; E-mail: palmoro@nip.upd.edu.ph

1 Introduction

Ubiquitous in optical metrology, fringe patterns are comprised of dark and bright contour-like structures representing interferograms, absolute phases or phase difference maps. Fringe analysis involves various methods for qualitative and quantitative evaluations with the aim of correlating the fringe pattern with the actual physical information such as object location, shape, deformation, or change in the index of refraction or sensitivity vector [1]. The various methods may be categorized based on spatial feature analyzed, type of fringes and number of images used to extract the phase. Early methods were focused at fringe center extraction, fringe order counting and sub-fringe interpolation. There were methods specific for contour-type and for carrier-type fringe patterns. To extract the phase, multiple images may be used such as in phase-

SPECKLE 2015: VI International Conference on Speckle Metrology, edited by Fernando Mendoza Santoyo, Eugenio R. Méndez, Proc. of SPIE Vol. 9660, 96600F · © 2015 SPIE · CCC code: 0277-786X/15/$18 · doi: 10.1117/12.2196757